Talanta 99 (2012) 302–309

Contents lists available at SciVerse ScienceDirect

Talanta

journal homepage: www.elsevier.com/locate/talanta

An amperometric bienzymatic cholesterol biosensor based on functionalized graphene modified electrode and its electrocatalytic activity towards total cholesterol determination

Revanasiddappa Manjunatha [a], Gurukar Shivappa Suresh [a,*], Jose Savio Melo [b], Stanislaus F. D'Souza [b], Thimmappa Venkatarangaiah Venkatesha [c]

[a] Chemistry Research Centre, S. S. M. R. V. Degree College, Jayanagar, Bangalore-560041, India
[b] Nuclear Agriculture and Biotechnology Division, Bhabha Atomic Research Centre, Mumbai-400085, India
[c] Department of Chemistry, Kuvempu University, Jnanasahyadri, Shimoga-577451, India

ARTICLE INFO

Article history:
Received 9 April 2012
Received in revised form
24 May 2012
Accepted 25 May 2012
Available online 1 June 2012

Keywords:
Direct electrochemistry
Cholesterol oxidase
Cholesterol esterase
Hydrogen peroxide
Total cholesterol

ABSTRACT

Cholesterol oxidase (ChOx) and cholesterol esterase (ChEt) have been covalently immobilized onto functionalized graphene (FG) modified graphite electrode. Enzymes modified electrodes were characterized using cyclic voltammetry (CV) and electrochemical impedance spectroscopy (EIS). FG accelerates the electron transfer from electrode surface to the immobilized ChOx, achieving the direct electrochemistry of ChOx. A well defined redox peak was observed, corresponding to the direct electron transfer of the FAD/$FADH_2$ of ChOx. The electron transfer coefficient (α) and electron transfer rate constant (K_s) were calculated and their values are found to be 0.31 and 0.78 s^{-1}, respectively. For the free cholesterol determination, ChOx-FG/Gr electrode exhibits a sensitive response from 50 to 350 μM ($R=-0.9972$) with a detection limit of 5 μM. For total cholesterol determination, co-immobilization of ChEt and ChOx on modified electrode, i.e. (ChEt/ChOx)-FG/Gr electrode showed linear range from 50 to 300 μM ($R=-0.9982$) with a detection limit of 15 μM. Some common interferents like glucose, ascorbic acid and uric acid did not cause any interference, due to the use of a low operating potential. The FG/Gr electrode exhibits good electrocatalytic activity towards hydrogen peroxide (H_2O_2). A wide linear response to H_2O_2 ranging from 0.5 to 7 mM ($R=-0.9967$) with a sensitivity of 443.25 μA mM^{-1} cm^{-2} has been obtained.

1. Introduction

Graphene is a new class of two dimensional sheet material, with an extraordinary electronic transport property. Uniqueness and versatility of graphene is due to its physical and chemical properties such as high surface area, ease of functionalization and simple production. Graphene provides an ideal platform to prepare biosensors [1,2]. The surface of graphene possesses greater sp^2 character than single walled carbon nanotubes (SWCNTs) and conductivity of the graphene is estimated to be about 64 mS cm^{-1}, which is about approximately sixty times better than that of SWCNTs [3]. Graphene modified electrodes showed better conductivity and electrocatalytic activity than those of multiwalled carbon nanotubes (MWCNTs) because of two dimensional structure and unique electronic property [4]. Even though graphene possesses excellent electrocatlytic activity and is a novel material for electrode modification, it will ascertain many of the unique and excellent properties only when it is integrated into complex assemblies [5,6]. Chemical functionalization of graphene is a useful technique to incorporate graphene into such assemblies, in which covalent bonding between material of interest and functionalized graphene takes place. This is also useful for improving dispersion and homogeneity of graphene in organic and aqueous solvents [7,8].

Determination of cholesterol is very important in clinical diagnosis because its level in blood is closely related to human health. In fact high cholesterol level in blood increases the risk of clinical disorders such as hypertension, stroke, myocardial infarction, cerebral thrombosis, coronary and peripheral vascular diseases [9]. Traditionally, cholesterol was measured using non-enzymatic spectrometry, via the production of colored substances, like cholestapolyenes and cholestapolyene carbonium ions (Liebermann-Burchard reaction). This method suffered from poor specificity, instability of the color reagents, standardization difficulties and corrosive nature of the reagent used [10]. So, it is very essential to develop a fast, sensitive and selective way to

* Corresponding author. Tel.: +91 80 26654920; fax: +91 80 22453665.
E-mail address: sureshssmrv@yahoo.co.in (G. Shivappa Suresh).

0039-9140/$ - see front matter © 2012 Elsevier B.V. All rights reserved.
http://dx.doi.org/10.1016/j.talanta.2012.05.056

measure cholesterol in biological samples. Amperometric cholesterol biosensors have been considered to be the most suitable devices due to their good selectivity, sensitivity, fast response, and reproducible results [11].

Electrochemical biosensors using desired enzyme immobilized on electrodes have become popular for detection of biological substances, because of ease of preparation, high sensitivity and specificity of electrochemical biosensors. The most critical step involved in the preparation of electrochemical biosensors is the immobilization of enzyme onto the electrode surface. Cholesterol esterase (ChEt) known as bile salt-activated lipase, catalyzes the hydrolysis of dietary cholesterol esters, triacylglycerols phospholipids and vitamin esters via a serine protease mechanism. Cholesterol oxidase (ChOx) is a flavin-adenine-dinucleotide (FAD) containing flavoenzyme. In the presence of oxygen, ChOx catalyzes two reactions; oxidation of cholesterol to cholest-5-en-3-one and subsequently the isomerization to cholest-4-en-3-one [12]. The commonly used methods for immobilization of ChOx enzymes are entrapment [13], physical adsorption [14] and covalent binding using cross linkers [15]. The later method has been employed to improve uniformity, density and distribution of the bound protein as well as reproducibility on the electrode surface [16].

Direct electron transfer [DET] of redox proteins not only provides a model for the study of electron transport of proteins in biological systems, which is important to understand the material metabolism and energy transformation in life processes, but also establishes a foundation for the fabrication of third generation of electrochemical biosensors [17]. The DET of enzymes on an electrode is generally difficult since the enzyme active sites are deeply buried in the protein matrix. To achieve DET, efforts have been devoted to designing biocompatible matrix to retain the native structure of the redox enzymes [18]. From the literature it is confirmed that, several studies have been performed on DET of glucose oxidase, horseradish peroxidase and hemoglobin [19–21]. However, there have been only a few reports on the DET of ChOx [22–25]. To the best of our knowledge, for the first time, we are reporting the DET of ChOx using graphite electrode modified with carboxylic functionalized graphene.

In the present study, functionalized graphene was prepared and used for the modification of Graphite (Gr) electrode. The biosensor is constructed using the enzymes ChOx and ChEt, for free and total cholesterol determination on FG/Gr electrode. The FG modified electrode showed low potential and sensitive detection of H_2O_2 than the bare graphite electrode. The enzyme modified electrode was characterized using cyclic voltammetry and electrochemical impedance spectroscopy. It was found that the carboxylic functionalized graphene can provide a favorable microenvironment for ChOx to realize DET.

2. Experimental details

2.1. Reagents

Cholesterol esterase, Triton X-100, isopropanol, cholesterol, cholesterol palmitate and nonaethylene glycol monododecyl ether were procured from Sigma Aldrich. Cholesterol oxidase, glutaraldehyde and bovine serum albumin (BSA) were procured from SRL, India. Hydrogen peroxide (30 wt%) was purchased from Merck. Graphene was purchased from Quantum Materials, India. $-COO^-$ groups were introduced on graphene by refluxing with conc. HNO_3 for 5 h. Phosphate buffer saline of pH 7. 0 (PBS) was prepared from stock solutions of 0.1 M KH_2PO_4, 0.1 M K_2HPO_4 and 0.1 M KCl. All other chemicals used were of analytical reagent grade unless otherwise mentioned and used without further purification. All solutions were prepared with double distilled water.

2.2. Enzyme solution preparation

100 U/ml ChOx and 150 U/ml ChEt solutions were prepared in 0.1 M PBS of pH 7.0. A stock solution of 10 mM cholesterol was prepared by dissolving 0.0967 g of cholesterol in a mixture of 1 ml Triton X-100 and 0.5 ml isopropanol at 65 °C and diluting the resulting solution to 25 mL in a standard flask using hot PBS of pH 7.0. The solution was stored at 4 °C in the dark and was stable for two weeks (until a slight turbidity was observed). A stock solution of 10 mM cholesterol palmitate was prepared by dissolving 0.156 g of cholesterol palmitate in nonaethylene glycol monododecyl ether at 65 °C. Then hot PBS was added and volume made upto 25 ml.

2.3. Electrochemical measurements

Cyclic voltammetry and electrochemical impedance spectroscopy experiments were carried out with Versa stat 3 (Princeton Applied Research, USA). Raman scattering measurements were carried out using a diamond anvil cell (DAC) Diacell Products, UK, model B-05 with octagonal diamonds 400 μm diameter culet. The 532 nm laser line is used to excite the Raman spectrum and the power on the sample was 15 mW. Scattered light was analyzed by a 0.9 m single monochromator [26] coupled with a super-notch filter and detected using a cooled CCD (Andor Technology). Resolution limited line width at 550 nm is measured to be about 2 cm^{-1} for an entrance slit opening of 50 μm. Transmission electron microscopy (TEM) was performed using a Carl Zeiss instrument. All experiments were done in a three electrode electrochemical cell with a bare graphite electrode or modified graphite electrode as working electrode, saturated calomel as reference electrode (SCE) and platinum wire as auxiliary electrode.

2.4. Preparation of modified graphite electrode

An electrode was fabricated by inserting a 6 mm diameter graphite cylinder in the hole of a Teflon bar with the same internal diameter; contact was made with copper wire through the center of the Teflon bar. The electrode was polished with emery paper of different grades i.e. 1000, 800, 6/0, 4/0, and finally with 2/0 until a mirror shining surface was obtained and finally rinsed with double distilled water in an ultrasonic bath for several minutes. A complete investigation on the chemical composition and physical properties of graphene decorated with carboxylic groups reveals that they are well dispersed in aqueous medium for several months. Such long term stability is due to negatively charged functional groups present in the graphene [27,28]. Further, we can attach or decorate desired functional moiety on the graphene containing negatively charged carboxylic groups. It is also helpful to develop multilayer of oppositely charged species on the negatively charged functionalized graphene. Thus in the present study $-COO^-$ groups were introduced on graphene by refluxing with conc. HNO_3 for 5 h. Functionalized graphene modified graphite electrode (FG/Gr) was prepared by using the following procedure. First, 10 mg functionalized graphene (FG) was dispersed in 1 ml double-distilled water, ultrasonicated for 15 minutes to give a 10 mg/ml black suspension. Then, 12 μL of 10 mg/ml FG suspension was dropped on the surface of graphite electrode and dried under ambient temperature. This modified electrode is denoted as FG/Gr electrode and used for the detection of hydrogen peroxide (H_2O_2).

2.5. Preparation of enzyme modified electrode

10 μL of glutaraldehyde (2.5% w/w) and 20 μL of bovine serum albumin (BSA) (30 mg/ ml in PBS pH 7.0) were mixed together and 5 μL of the resulting solution was placed onto the FG/Gr electrode and dried at room temperature. 8 μL of ChOx was dropped onto the

glutaraldehyde-BSA modified FG/Gr electrode surface and dried at 4 °C. Resulting electrode is denoted as ChOx-FG/Gr, which is used for detection of free cholesterol. Similarly 10 μL of ChOx and 5 μL of ChEt were mixed together and 8 μL of the resulting solution was placed onto the glutaraldehyde-BSA modified FG/Gr electrode surface and dried at 4 °C. Resulting electrode is denoted as (ChEt/ChOx)-FG/Gr, which is used for detection of total cholesterol. The enzyme-modified electrodes were stored in 0.1 M PBS, pH 7.0 at 4 °C in a refrigerator when not in use.

3. Results and discussion

3.1. Characterization of functionalized graphene

Raman spectroscopy is a powerful nondestructive tool for characterizing carbonaceous materials, particularly to differentiate ordered and disordered crystal structures of carbon. Fig. 1A shows the Raman spectra of pristine graphene (curve a) and functionalized graphene (curve b). The two peaks are attributed to the G band at ~1574 cm^{-1} and D band at ~1341 cm^{-1}, respectively, which is in good agreement with what has been previously reported [29]. The G band corresponds to an E_{2g} mode of graphene and it is related to vibration of sp^2-bonded carbon atoms in a two-dimensional hexagonal lattice. The D-band is related to disorder-induced scattering resulting from imperfections or loss of hexagonal symmetry of disordered graphene. The intensity ratio of the D and G bands (I_D/I_G) is commonly used to evaluate the amount of structural defects and as a quantitative measure of edge plane exposure. I_D/I_G ratio of functionalized graphene was found to be 1.09, whereas it was 0.84 for pristine graphene. The larger I_D/I_G ratio for the functionalized graphene is on account of the structural defects due to the incorporation of carboxylic groups at the edges of graphene. Fig. 1B shows TEM images of the pristine graphene (a) and functionalized graphene sheets (b). In both the images wrinkles are observed. These wrinkles could be important for preventing aggregation of graphene due to Van der Waals forces during drying and maintaining high surface area [30].

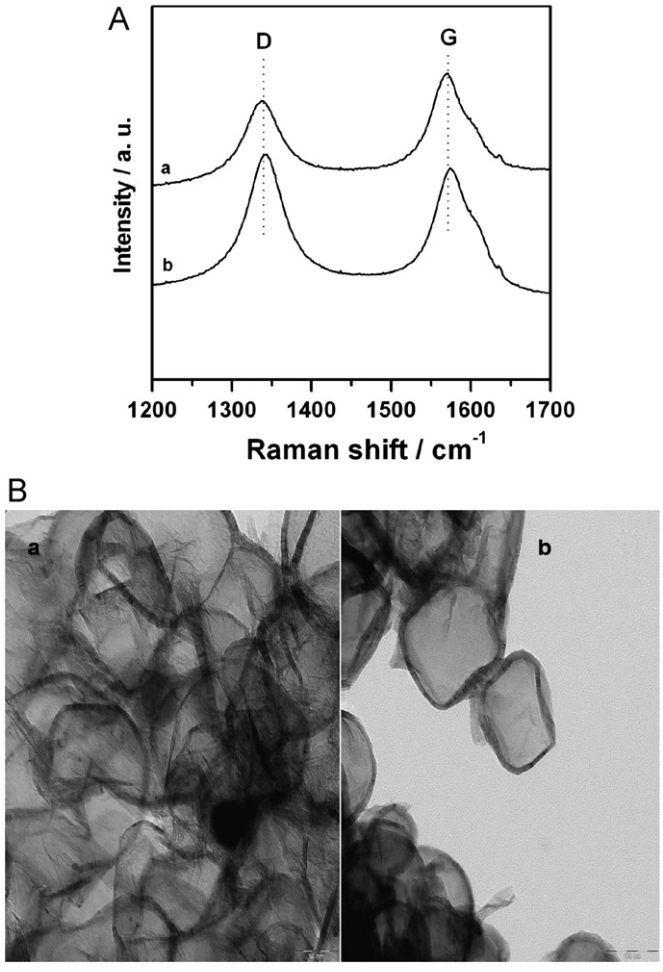

Fig. 1. (A) Raman spectra of pristine graphene (a) and functionalized graphene (b). (B) TEM image of pristine graphene (a) and functionalized graphene (b).

3.2. Characterization of modified electrodes using cyclic voltammetry (CV) and electrochemical impedance spectroscopy (EIS)

The cyclic voltammeric behavior of bare graphite electrode and FG modified electrode was studied using 1 mM $Fe(CN)_6^{3-/4-}$ as an electrochemical probe in PBS, pH 7.0 containing 0.1 M KCl as shown in Fig. 2A. The cyclic voltmmogram of bare graphite electrode in 1 mM $Fe(CN)_6^{3-/4-}$ shows quasi-reversible peak with a peak to peak separation (ΔE_p) of 146 mV. The higher ΔE_p value could be due to the redox kinetics of $Fe(CN)_6^{3-/4-}$ being affected when the K^+ concentration in the electrolyte is changed. The K^+ ions in the electrolyte act as a bridge between the electrode surface and the redox moiety present in the solution. The electrochemical kinetics is better at higher concentration of K^+ than at lower concentrations. Therefore redox kinetics of $Fe(CN)_6^{3-/4-}$ is reported to be affected by the nature and concentration of the supporting electrolyte [31–33]. Ramesh et al. [31] found ΔE_p for the $Fe(CN)_6^{3-/4-}$ redox probe at electrode to be 210 mV, when they used 0.1 M potassium phosphate buffer. However, ΔE_p decreases with the increase in the strength of potassium phosphate buffer. Thus, in our studies, ΔE_p for the graphite and modified graphite electrodes in $Fe(CN)_6^{3-/4-}$ was found to be 146 and 133 mV at the scan rate of 100 mVs^{-1}. This could be due the strength of potassium phosphate buffer (0.1 M) used for the study. After immobilization of ChOx enzyme on FG/Gr electrode, ΔE_p increases to 187 mV along with decrease in the peak current of redox probe. This could be due to presence of macromolecular, bulky structure of ChOx, which could hinder the electron transfer of $Fe(CN)_6^{3-/4-}$ to the electrode surface.

Characterization of modified electrodes was further investigated using EIS. This is a powerful and sensitive characterization tool for studying the charge transfer process at electrode/electrolyte interface [34]. EIS was carried out in the presence of 1 mM $Fe(CN)_6^{4-/3-}$ as a redox probe, in the frequency range of 100 kHz to 0.1 Hz with amplitude of 5 mV as shown in Fig. 2B. It seems that the impedance responses of electrodes are quite complex and include some adsorption processes. The simulated curve of experimental data and best fitting Randles equivalent circuit are shown in the Fig. 2C. The values of charge transfer resistance (R_{ct}), solution resistance (R_s), Warburg impedance (W) and double layer capacitance (C_{dl}) were obtained by fitting the Randles equivalent circuit to the experimental data. The obtained impedance values are shown in Table 1. The R_{ct} of FG/Gr electrode (curve b) is much less as compared to bare graphite electrode (curve a), which is due to the presence of FG. This promotes the kinetics of electron transfer process towards the electrode. After immobilization of ChOx enzyme (curve c), R_{ct} increases even though the semicircle is not properly seen, probably as the semicircle is replaced with a straight sloping line when R_{ct} is very high [35,36]. This is due to the non-conducting nature of enzyme.

3.3. Electrocatalytic activity of FG/Gr electrode towards H_2O_2

The electrocatalytic property of FG/Gr electrode towards H_2O_2 was studied using CV. Fig. 3 presents the CVs in the absence and presence of 6 mM H_2O_2, recorded at bare graphite and FG/Gr electrodes at the scan rate of 25 mVs^{-1}. Only a small reduction

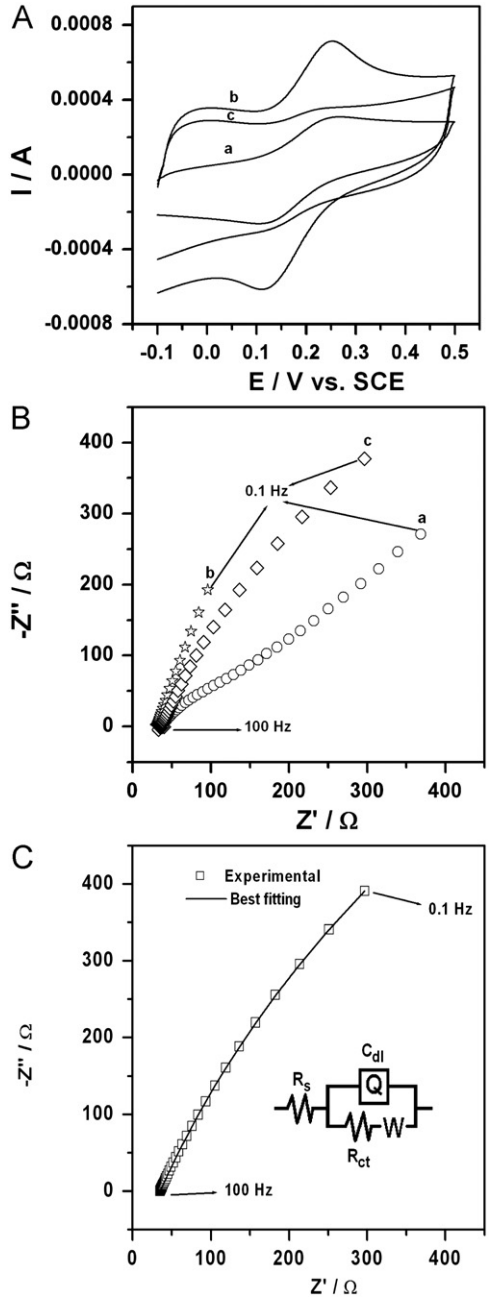

Fig. 2. (A) Cyclic voltammograms of bare graphite (a), FG/Gr electrode (b) and ChOx-FG/Gr electrode (c) in 0.1 M PBS (pH 7.0) containing 1 mM $Fe(CN)_6^{4-/3-}$ Scan rate 100 mVs^{-1}. (B) Nyquist impedance plots of bare graphite (a), FG/Gr electrode (b) and ChOx-FG/Gr electrode (c). The frequency range is from 100 kHz to 0.1 Hz and amplitude 5 mV. The supporting electrolyte is 0.1 M PBS containing 0.1 M KCl (pH 7.0). (C) Nyquist impedance plots of experimental data of ChOx-FG/Gr electrode and best fitting by using Randles equivalent circuit shown in inset.

Table 1
EIS data of bare Gr, FG/Gr and ChOx-FG/Gr electrodes in 1 mM $Fe(CN)_6^{3-/4-}$.

Electrode	R_s (Ω)	n	Q (mF)	R_{ct} (Ω)	W (Ω)
Bare Gr	37.5	0.8	0.74	154.6	0.0028
FG/Gr	30.5	0.8	6.85E-5	0.01	0.0003
ChOx-FG/Gr	33.39	0.73	4.12E5	2455	4.12 E5

current was observed at the bare graphite electrode (curve b), while FG/Gr electrode has significant electrocatalytic activity towards reduction of H_2O_2. A sharp peak appeared at −400 mV

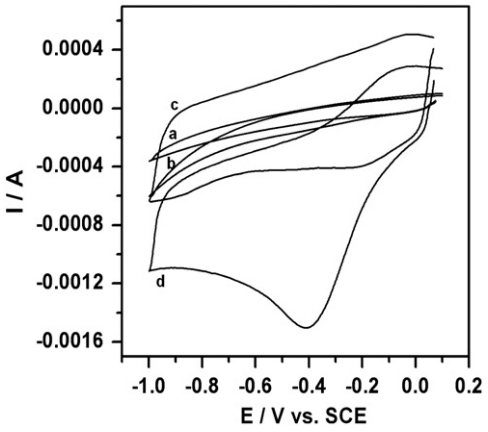

Fig. 3. Cyclic voltammograms of bare graphite (a, b) and FG/Gr electrode (c,d) in the absence of (a, c) and presence of (b, d) 6 mM H_2O_2 in 0.1 M PBS (pH 7.0) scan rate 25 mVs^{-1}.

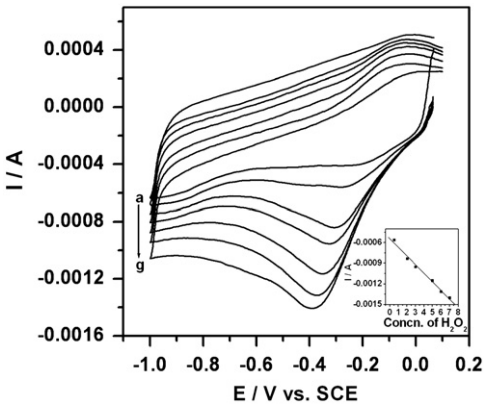

Fig. 4. CV curves of FG/Gr electrode recorded in 0.1 M PBS (pH 7.0) (a) and successive addition of various concentrations of H_2O_2 (0.5, 2, 3, 5, 6 and 7 mM) (b–g). Scan rate 25 mVs^{-1}. Inset shows the relationship between current density of H_2O_2 reduction vs. concentrations.

and about 10 fold increase in reduction peak current was observed at FG/Gr electrode (curve d), as compared to bare graphite electrode. This may be attributed to the large surface area and enhanced electron transfer ability of FG.

3.4. Effect of scan rate and increasing concentration of H_2O_2 at FG/Gr electrode

The effect of scan rate on cathodic peak potential and peak current of H_2O_2 was performed using CV studies. The cyclic voltammograms at different scan rates from 5 to 250 mV s^{-1} of FG/Gr electrode were obtained in 0.1 M PBS of pH 7.0 containing 5 mM H_2O_2 (Figure not shown). With the increase in scan rate, cathodic peak currents of the modified electrode increased and the peak potential shifted to more negative values. Cathodic peak currents are found to be linearly proportional to the square root of the scan rate, suggesting the electrochemical reaction of H_2O_2 at FG/Gr electrode is a diffusion-controlled process [37].

The CVs of FG/Gr electrode in different concentrations of H_2O_2 was investigated. As shown in Fig. 4, the cathodic peak current increases linearly with the addition of H_2O_2, this shows the catalytic reduction of H_2O_2. The linear relationship between cathodic peak current and H_2O_2 concentration was obtained in the range of 0.5–7 mM with a sensitivity of 124.11 μA mM^{-1} (or 443.25 μA mM^{-1} cm^{-2}). The linear regression equation is

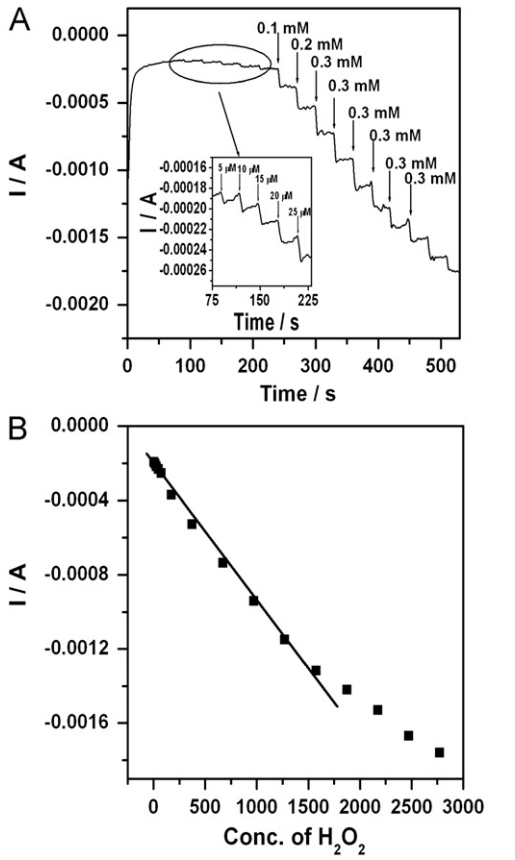

Fig. 5. Current density-time response curve of H_2O_2 reduction obtained at FG/Gr electrode with successive addition of various volumes and concentrations of H_2O_2 into 0.1 M PBS (pH0). applied potential: −350 mV. The solution was stirred using magnetic pallet during measurement. Inset shows the magnification of the oval part. (B) Plot of current density of H_2O_2 reduction vs. concentrations.

given as follows:

$$I_{pc(H_2O_2)}(\mu A) = -5.5257E{-}4 - 1.2411E{-}4C_{(H_2O_2)}(\mu A);\quad R = -0.9967 \tag{1}$$

Amperometry is one of the most widely used techniques for evaluating sensors. Fig. 5A. shows the amperometric response on the successive increments of H_2O_2 of various concentrations, added in stirred PBS solution, at an applied potential of −350 mV. A stepwise growth of reduction current can be observed with increasing amount of H_2O_2. Modified electrode achieved steady-state signals within 3 s, indicating a fast diffusion of substrate into the modified electrode. This is much less than those based on ta-C:P/Au electrode; 8 s [37], Cuo-nanoflower-modified electrode; 10 s [38], Co_3O_4/GCE; 10 s [39], PANI-g-MWNT-ME; 8 s [40], PANI/SWCNTs/Pt electrode; 4 s [41]. The modified electrode exhibits linear response to the concentrations in the range of 5 μM–1.575 mM with a detection limit of 1.6 μM. The linear characteristics of the modified electrode for H_2O_2 is shown in Fig. 5B. The linear regression equation is given as follows:

$$I_{pc(H_2O_2)}(\mu A) = -2.1159E{-}4 - 7.2997E{-}4C_{(H_2O_2)}(\mu A);\quad R = -0.9978 \tag{2}$$

3.5. Direct electron transfer of ChOx-FG/Gr electrode

The excellent performance of FG/Gr electrode towards the detection of H_2O_2 makes it attractive for the fabrication of oxidase-based biosensors. Cholesterol oxidase was selected as a model enzyme. Fig. 6 shows CVs of bare graphite electrode (curve a), FG/Gr electrode (curve b) and ChOx/FG/Gr electrode (curve c). When ChOx enzyme was immobilized on FG/Gr electrode, a pair of stable and well defined peaks of ChOx for the FAD/$FADH_2$ redox couple transformation were observed, which could be ascribed to electron transfer between ChOx and underlying electrode [22–25]. The anodic and cathodic peak potential was found to be −0.45 and −0.532 V respectively. The potential difference between the two peaks ΔE_p was 82 mV at a scan rate of 100 mVs^{-1}, which suggests that ChOx has undergone a quasi-reversible redox reaction at modified electrode. The surface area τ of ChOx/FG/Gr electrode was calculated using the following equation:

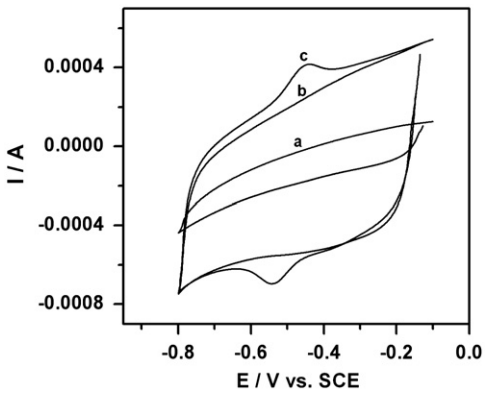

Fig. 6. Cyclic voltammograms of of bare graphite (a), FG/Gr electrode (b) and ChOx-FG/Gr electrode in 0.1 M PBS (pH 7.0) scan rate: 100 mVs^{-1}.

$$\tau = Q/nFA \tag{3}$$

where, Q is the charge, n is the number of electrons transferred, F is the Faraday constant. Therefore τ was found to be 1.406×10^{-8} mol cm^{-2}, which indicates that large amount of enzyme could be immobilized onto FG, because of its large surface area.

The influence of the scan rates on the cyclic voltammetric performance of the ChOx-FG/Gr electrode was investigated. The anodic and cathodic peak currents varied linearly with the scan rate between 25 and 250 mVs^{-1} (Figure not shown). The linear regression equations are as given below.

$$I_{pa} = -6.1436E{-}4 + 0.0036v(Vs^{-1});\ R = 0.9982 \tag{4}$$

$$I_{pc} = -1.5206E{-}4 - 0.00418v(Vs^{-1});\ R = 0.9985 \tag{5}$$

In the scan rate ranging from 100 to 400 mVs^{-1}, the linear regression equations of E_{pa} and E_{pc} vs. logarithm of the scan rates are expressed as

$$E_{pa} = -0.6137 + 0.09674\log v(Vs^{-1});\ R = 0.9982 \tag{6}$$

$$E_{pc} = -0.3275 - 0.1054\log v(Vs^{-1});\ R = 0.9986 \tag{7}$$

The electron-transfer coefficient (α) was found to be 0.31, based on the slopes of the line $2.3RT/(1-\alpha)nF$ and $-2.3RT/\alpha nF$ for the anodic and cathodic peaks respectively. The electron transfer rate constant (K_s) was calculated to be 0.78 s^{-1}, using the following Laviron's equation [42]:

$$\log K_s = \alpha\log(1-\alpha) + (1-\alpha)log\ \alpha - log\left(\frac{RT}{nFv}\right) - \frac{\alpha(1-\alpha)nF\Delta Ep}{2.3RT} \tag{8}$$

The redox peaks of the ChOx enzyme should be affected by changing pH of the solution because of involvement of the protons in the overall electrode reaction. The influence of solution pH on redox reaction of ChOx on the ChOx-FG/Gr electrode was studied in the pH range 4.0– 10.0. As can be seen in Fig. 7A, the

solution pH obviously influenced the redox peak currents of the ChOx enzyme. The anodic and cathodic maximum peak currents and also highest reversibility of the enzyme was found at pH 7.0 (Fig. 7B). At higher or lower pHs, enzyme activity is less, which could be due to deactivation/leaching of enzyme from the electrode surface. The solution pH also influenced redox peak potentials of enzyme. As solution pH increases redox peak potentials of enzyme shifted negatively as shown in Fig. 7C, indicating that protons are involved in the redox reaction. A good linear relationship was obtained between half wave potential ($E_{1/2}$) and the solution pH. The linear regression equation is given as

$$E_{1/2} = -0.1277 - 0.0533\text{pH};\ R = 0.9990 \quad (9)$$

From the above equation, slope of $E_{1/2}$ is 53. 3 mV, which is close to the theoretical value (59 mV pH^{-1}) for a classical Nernstian two electrons and protons process. Hence, ChOx redox system is a two proton participated two electron redox process. The results of ChOx-FG/Gr electrode variation of anodic peak currents, peak potentials and half wave potentials at different pHs of the solution, are shown in Table 2.

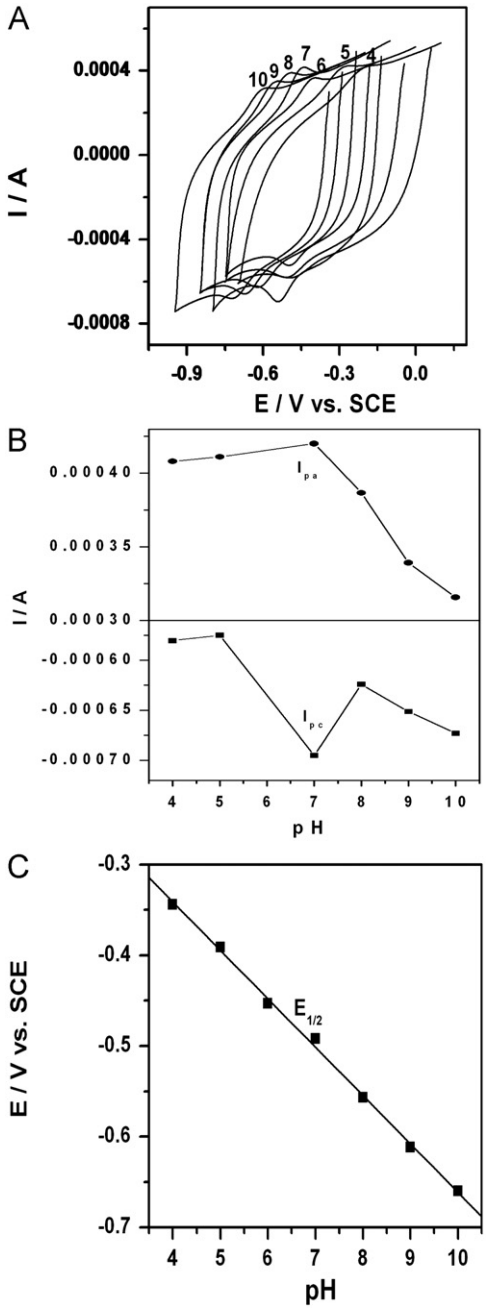

Fig. 7. (A) CVs of ChOx-FG/Gr electrode at various pHs of the solution (pH 4–10) scan rate: 100 mVs^{-1}. (B) Relationship between anodic peak current (I_{pa}), cathodic peak current (I_{pc}) with pH.

3.6. Determination of free and total cholesterol

As mentioned earlier, due to the high sensitivity and lower potential detection of H_2O_2 at FG/Gr electrode, a cholesterol biosensor was developed using enzymes ChOx and ChEt. ChOx was used for the free cholesterol determination and both the enzymes ChOx and ChEt, were used for total cholesterol determination, in which ChEt hydrolyzes cholesterol ester to cholesterol and ChOx catalyzes oxidation of cholesterol. Fig. 8A and B show amperometric responses of ChOx-FG/Gr and (ChEt/ChOX)-FG/Gr electrodes to the addition of 50 μM cholesterol and cholesterol palmitate respectively, at an applied potential of −350 mV.

Table 2
Cyclic voltametric response of ChOx-FG/Gr electrode at different solution pH.

pH	I_{pa}/A	I_{pc}/A	E_{pa} vs SCE	E_{pc} vs SCE	$E_{1/2}$ vs SCE
4	4.08E-4	−5.80E-4	−0.214	−0.475	−0.344
5	4.11E-4	−5.75E-4	−0.290	−0.493	−0.391
6	3.58E-4	−5.21E-4	−0.411	−0.496	−0.453
7	4.20E-4	−6.95E-4	−0.451	−0.534	−0.492
8	3.86E-4	−6.24E-4	−0.501	−0.614	−0.557
9	3.39E-4	−6.51E-4	−0.559	−0.660	−0.612
10	3.15E-4	−6.73E-4	−0.606	−0.714	−0.660

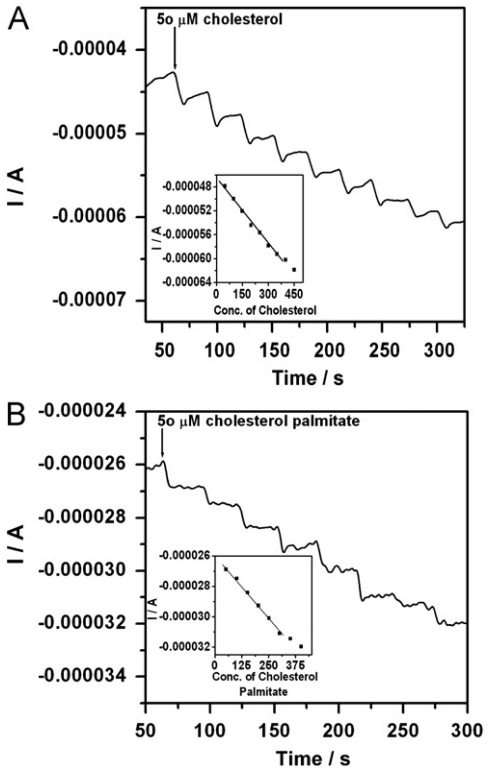

Fig. 8. (A) Amperometric response of ChOx-FG/Gr electrode for each addition of 50 μM cholesterol at constant applied potential −350 mV in PBS containing 0.1 M KCl (pH 7.0). Inset shows relationship between cathodic peak current (I_{pc}) and concentrations of cholesterol. (B) Amperometric response of (ChEt/ChOx)-FG/Gr electrode for each addition of 50 μM cholesterol palmitate at constant applied potential −350 mV in PBS containing 0.1 M KCl (pH 7.0). Inset shows relationship between cathodic peak current (I_{pc}) and concentrations of cholesterol palmitate.

Reduction current increases obviously after addition of cholesterol and cholesterol palmitate. This shows that ChOx and ChEt have bioactive property on FG/Gr electrode. Usually, the response of ChOx biosensor is slow and a response time of about 1 min is needed [43,44]. However, ChOx-FG/Gr and (ChEt/ChOX)-FG/Gr electrodes achieved steady state signal within 9 and 12 s, respectively, which could be due to electrocatalytic property of FG towards reduction of H_2O_2 which was produced during the course of enzymatic reaction. The linear range of above mentioned electrodes were 50–350 μM and 50–300 μM with the detection limits of 5 and 15 μM respectively. The linear regression equation is expressed as follows:

$$I_{pc(Cholesterol)}(\mu A) = -4.6241E{-}5 - 3.8164E{-}4C_{(Cholesterol)}(\mu A); \quad R = -0.9972 \tag{10}$$

$$I_{pc(Cholesterol\ Palmitate)}(\mu A) = -2.5869E{-}5 - 1.7024E{-}4C_{(Cholesterol\ Palmitate)}(\mu A); R{-}0.9982 \tag{11}$$

Comparison of the ChOx enzyme modified electrode with other ChOx based biosensors are given in Table 3 [22–25,45,46]. From the table it is clear that, the functionalized graphene modified electrode could provide large surface area to accommodate ChOx enzyme compared to MWCNTs modified bioelectodes. Also electron transfer rate constant (K_s), applied potential and linear range of the functionalized graphene modified electrode are found to be good with respect to other nanoparticle modified electrodes [22,25,45]. Determination of free and total cholesterol on enzyme modified electrode was carried out at an applied potential of −350 mV. The common interferents such as ascorbic acid, uric acid and glucose could not cause any interference because the applied potential was too low for oxidation of these interferents (Fig. not shown). Fig. 9 shows ten consecutive CV curves of ChOx-FG/Gr electrode in 0.1 M PBS pH 7.0 at scan rate of 100 mVs^{-1}. It can be seen that attachment of ChOx onto the FG by means of glutaraldehyde as cross-linker is very stable upon repeated potential cycling, with almost no change in both the peak current and peak to peak separation. Thus enzyme modified electrode showed good stability. Similarly, to ascertain fabrication reproducibility, three sets of ChOx-FG/Gr and (ChEt/ChOx)-FG/Gr were fabricated for the determination of free and total cholesterol respectively. The results revealed that the amperomtric biosensors had very satisfying reproducibility with the relative standard deviation (RSD) of 4.6 and 4.8%.

3.7. Determination of free and total cholesterol in serum samples

For practical applications, the analysis of free and total cholesterol in serum sample is important. For this reason, ChOx-FG/Gr and (ChEt/ChOx)-FG/Gr electrodes were used for the determination of free and total cholesterol in the serum samples by amperometric technique. The serum samples were diluted in such a way that, cholesterol concentrations should fall in the working range of above mentioned electrodes. The current response from each serum sample at an applied potential of −350 mV was measured. The free and total cholesterol were then determined by interpolation on the linear range of calibration curves of standard free and total cholesterol. The values obtained from the enzyme electrodes were compared with standard spectrophotometric method as shown in Table 4. The results obtained were satisfactory with the relative standard deviation ranging from 4.2 to 5.4%.

4. Conclusion

We have successfully fabricated a ChOx and ChEt enzymes based cholesterol biosensors for free and total cholesterol determination on FG/Gr electrode. The enzyme modified electrodes were characterized using CV and EIS. The results indicate that FG showed high electrocatalytic activity towards H_2O_2 and that it can provide a biocompatiable, favorable microenvironment for the enzymes and promote the direct electron transfer at the electrode surface. This could be due to FG having a high conductivity for electrochemical response and providing a significantly increased area for protein loading. The proposed amperometric biosensor exhibits good stability, sensitivity and fabrication reproducibility. The common interferents did not cause any interference due to the use of a low operating potential.

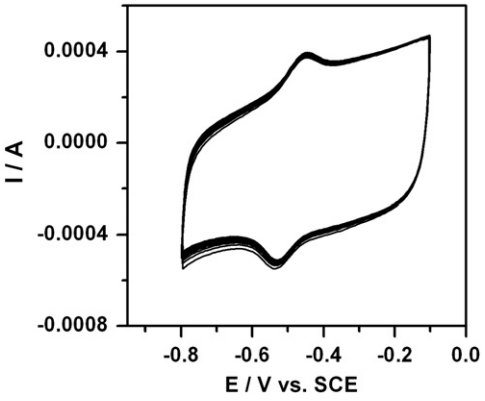

Fig. 9. Cyclic voltammogram of ten consecutive cycles of ChOx-FG/Gr electrode in 0.1 M KCl (pH 7.0) scan rate: 100 mVs^{-1}.

Table 4
Determination of free and total cholesterol in human serum samples (n=5) obtained at ChOx-FG/Gr and (ChEt/ChOx)-FG/Gr electrodes.

Sample No.	Biosensor method		R.S.D. (%)	Spectrophotometric method	
	Free cholesterol ($mmolL^{-1}$)	Total cholesterol ($mmolL^{-1}$)		Free cholesterol ($mmolL^{-1}$)	Total cholesterol ($mmolL^{-1}$)
1	2.25	4.78	4.9	–	4.90
2	1.82	4.92	4.2	–	4.75
3	2.05	4.35	5.4	–	4.56

Table 3
Comparison of the ChOx enzyme modified electrode with other ChOx based biosensors.

Cholesterol Biosensor	Γ mol cm^{-2}	Ks s^{-1}	Potential applied (mV)	Linear range (μM)	Detection limit (μM)	Reference
Chox/MWCNTs/GCE	1.86×10^{-11}	0.029	−800	46.8–279	46.8	[22]
Chox/KMWCNTs/GCE	1.46×10^{-10}	2.80	−500	0.05–16	0.005	[23]
MP/Chox/AUNPs-GSH/PDATT/GCE	5.8×10^{-11}	0.75	−300	10–130	0.3	[25]
GNS-nPt/SPE	–	–	400	0–35	0.2	[45]
SP-rhodium-graphite-Au-P450scc	–	–	−400	10–70	–	[46]
ChOx-FG/Gr	1.406×10^{-8}	0.78	−350	50–350	5	Present work

Acknowledgments

The authors gratefully acknowledge the financial support from Department of Atomic Energy-Board of Research in Nuclear Sciences (DAE–BRNS), Government of India. We thank Sri. A.V.S. Murthy, honorary secretary, Rashtreeya Sikshana Samiti Trust, Bangalore and Dr. P. Yashoda, Principal, S. S. M. R. V. Degree college, Bangalore for their continuous support and encouragement. We also thank Dr. Anand Ballal, Molecular Biology Division, Bhabha Atomic Research Center, Mumbai for extending the facility of TEM and Dr. Rekha Rao, Solid State Physics Divison, Bhabha Atomic Research Center, Mumbai for Raman measurements.

References

[1] L.-M. Lu, H.-B. Li, F. Qu, X.-B. Zhang, G.-L. Shen, R.-Q. Tu, Biosensors Bioelectron. 26 (2011) 3500–3504.
[2] M. Mallesha, R. Manjunatha, C. Nethravathi, G.S. Suresh, M. Rajamathi, J.S. Melo, T.V. Venkatesha, Bioelectrochemistry 81 (2011) 104–108.
[3] S. Alwarappan, A. Erdem, C. Liu, C.-Z. Li, J. Phys. Chem. C 113 (2009) 8853–8857.
[4] S.P. Kumar, R. Manjunatha, C. Netravathi, G.S. Suresh, M. Rajamathi, T.V. Venkatesha, Electroanalysis 23 (2011) 842–849.
[5] J. Li, S. Guo, Y. Zhai, E. Wang, Anal. Chim. Acta 649 (2009) 196–201.
[6] C.L. Fu, W.S. Yang, X. Chen, D.G. Evans, Electrochem. Commun. 11 (2009) 997–1000.
[7] K.-J. Huang, D.-J. Niu, J.-Y. Sun, C.-H. Han, Z.-W. Wu, Y.-L. Li, X.-Q. Xiong, Colloids & Surf. B: Biointerfaces 82 (2011) 543–549.
[8] D. Li, R.B. Kaner, Science 320 (2008) 1170–1171.
[9] J. Maclachlan, A.T.L. Wotherspoon, R.O. Ansell, C.J.W. Brooks, J. Steroid Biochem. Mol. Biol. 72 (2000) 169–195.
[10] W. Richmond, Clin. Chem. 19 (1973) 1350–1356.
[11] S.P. Martin, D.J. Lamb, J.M. Lynch, S.M. Reddy, Anal. Chim. Acta 487 (2003) 91–100.
[12] A.K. Basu, P. Chattopadhyay, U. Roychoudhuri, R. Chakraborty, Bioelectrochemistry 70 (2007) 375–379.
[13] X. Tan, M. Li, P. Cai, L. Luo, X. Zou, Anal. Biochem. 337 (2005) 111–120.
[14] P.R. Solanki, S.K. Arya, S.P. Singh, M.K. Pandey, B.D. Malhotra, Sensors Actuators B 123 (2007) 829–839.
[15] A. Kumar, R.R. Pandey, B. Brantley, Talanta 69 (2006) 700–705.
[16] S.K. Arya, M. Datta, B.D. Malhotra, Biosensors Bioelectron. 23 (2008) 1083–1100.
[17] Z. Zhang, S. Chouchane, R.S. Magliozzo, J.F. Rusling, Anal. Chem. 74 (2002) 163–170.
[18] J.J. Feng, G. Zhao, J.J. Xu, H.Y. Chen, Anal. Biochem. 342 (2005) 280–286.
[19] C. Shan, H. Yang, J. Song, D. Han, A. Ivaska, Li Niu, Anal. Chem. 81 (2009) 2378–2382.
[20] F. Li, Y. Feng, Z. Wang, L. Yang, L. Zhuo, B. Tang, Biosens. Bioelectron. 25 (2010) 2244–2248.
[21] W. Ma, D. Tian, Bioelectrochem 78 (2010) 106–112.
[22] J.-Y. Yang, Y. Li, S.-M. Chen., K.-C. Lin, Int. J. Electrochem. Sci. 6 (2011) 2223–2234.
[23] X.-R. Li, J.-J. Xu, H.-Y. Chen, Electrochim. Acta 56 (2011) 9378–9385.
[24] R. Manjunatha, D.H. Nagaraju, G.S. Suresh, J.S. Melo, S.F. D'Souza, T.V. Venkatesha, J. Electroanal. Chem. 651 (2011) 24–29.
[25] A.A. Abdelwahab, M.S. Won, Y.B. Shim, Electroanalysis 22 (2010) 21–25.
[26] A.P. Roy, S.K. Deb, M.A. Rekha, A.K. Sinha, Indian J. Pure Appl. Phys. 30 (1992) 724.
[27] M.-C. Hsio, S.-H. Liao, M.-Y. Yen, P.-I. Liu, N.-M. Pu, C.-A. Wang, C.-C. Ma, ACS Appl. Mater. Interfaces 2 (2010) 3092–3099.
[28] E.-Y. Choi, T.H. Han, J. Hong, J.E. Kim, S.H. Lee, H.W. Kim, S.O. Kim, J. Mater. Chem. 20 (2010) 1907–1912.
[29] D. Geng, S. Yang, Y. Zhang, J. Yang, J. Liu, R. Li, T.-K. Sham, X. Sun, S. Ye, S. Knights, Appl. Surf. Sci. 257 (2011) 9193–9198.
[30] R. Kou, Y. Shao, D. Wang, M.H. Engelhard, J.H. Kwak, J. Wang, V.V. Viswanthan, C. Wang, Y. Lin, Y. Wang, I.A. Aksay, J. Liu, Electrochem. Comm. 11 (2009) 954–957.
[31] P. Ramesh, S. Bhagyalakshmi, S. Sampath, J, Colloid Interface Sci. 274 (2004) 95–102.
[32] E.L. Goldstein, M.R. Van DeMark, Electrochim. Acta 27 (1982) 1079–1085.
[33] R. Sohr, L. Muller, Electrochim. Acta 20 (1975) 451–455.
[34] A.J. Bard, L.R. Faulkerner, Electrochemical Methods Fundamentals and Applications, New York, Wiley-India Edition, 2006, p. 368–370.
[35] S.S. Zhang, K. Xu, T.R. Jow, J. Power Sources 115 (2003) 137–140.
[36] H. Manjunatha, T.V. Venkatesha, G.S. Suresh, Electrochim. Acta 58 (2011) 247–257.
[37] A. Liu, W. Dong, E. Liu, W. Tang, J. Zhu, J. Han, Electrochim. Acta 55 (2010) 1971–1977.
[38] M.-J. Song, S.W. Hwang, D. Whang, Talanta 80 (2010) 1648–1652.
[39] W. Jia, M. Guo, Z. Zheng, T. Yu, E.G. Rodriguez, Y. Wing, Y. Lei, J. Electroanal. Chem. 625 (2009) 27–32.
[40] P. Santhosh, K.M. Manesh, A. Gopalan, K.-P. Lee, Anal. Chem. Acta 575 (2006) 32–38.
[41] Q. Wang, Y. Yun, J. Zheng, Microchim. Acta 167 (2009) 153–157.
[42] E. Lavion, J. Electroanal. Chem. 101 (1979) 19–28.
[43] B. Sean, D. Dyer, G.E. Anthony, Biosensors Bioelectron. 17 (2002) 53–59.
[44] J.L. Besombes, S. Cosnier, P. Labbe, G. Revery, Anal. Chim. Acta 317 (1995) 275–280.
[45] R.S. Dey, C.R. Raj, J. Phys. Chem. C 114 (2010) 21427–21433.
[46] V. Shumyantseva, G. Deluca, T. Bulko, S. Carrara, C. Nicolini, S.A. Usanov, A. Archakov, Biosensors Bioelectron 19 (2004) 971–976.